# Fracture origins in $LiNbO_3$ wafers due to postprocessing micro-repolarization

Hirotoshi Nagata and Junichiro lchikawa
*Optoelectronics Research Division, New Technology Research Laboratories, Sumitomo Osaka Cement Co., Ltd., 585 Toyotomi-cho, Funabashi-shi, Chiba 274-8601, Japan*

Mitsuru Sakima
*Optoelectronics Division, New Technology Research Laboratories, Sumitomo Osaka Cement Co., Ltd., 585 Toyotomi-cho, Funabashi-shi, Chiba 274-8601, Japan*

Kaori Shima and Eungi Min Haga
*Advanced Materials Research Division New Technology Research Laboratories Sumitomo Osaka Cement Co., Ltd., 585 Toyotomi-cho, Funabashi-shi, Chiba 274-8601, Japan*

(Received 23 November 1998; accepted 5 April 1999)

In the process of developing electro-optic devices from ferroelectric z-cut $LiNbO_3$ wafers, a repolarization throughout the wafer thickness occurs due to a localization of electric charges on the wafer. The repolarization not only generates microdomains causing light to scatter but also large defects in the crystal that become the origin of wafer fracture. The size of such defects is comparable to the wafer thickness (0.5 mm), and an anomaly in the chemical and crystalline structures can be found in them. X-ray diffractometry and x-ray photoelectron spectroscopy confirm that a chemical reduction in the defective region occurs.

Since the worldwide expansion of optical fiber communication systems, the production of optical external modulators and other electro-optic waveguide devices made of ferroelectric $LiNbO_3$ crystalline wafers has proliferated.[1] High-speed optical phase modulators and optical polarization scramblers, in particular, are unique devices made from $LiNbO_3$. Z-cut $LiNbO_3$ wafers (i.e., crystallographic *c*-axis normal) are frequently used in the fabrication of such $LiNbO_3$ devices because they have the highest electro-optic constants and lowest dielectric constants.[2] The device fabrication process generally consists of a photolithograph of a waveguide pattern, a waveguide formation by Ti-indiffusion, a $SiO_2$ buffer layer deposition by the sputtering or evaporation technique, an oxygen-atmosphere annealing for the buffer layer, and an electro-plating of patterned electrodes.[3] Sometimes, a plasma etching of the surface is carried out to improve radio frequency performance.[4] But there is a disadvantage to using z-cut $LiNbO_3$ wafers; that is, at times, a postprocessing repolarization occurs during the fabrication process.[5] When observed through an optical microscope, this phenomenon appears as microdomains. Such repolarization can be atuibuted to extrinsic electrical charges on the wafer surface induced by the plasma process and the intrinsic charges caused by a pyro-effect of the crystal.

With respect to the optical performance of these devices, the prevalence of microdomains causes light to scatter, increasing the optical propagation loss of the waveguides. In addition to such problems, postprocessing repolarization may possibly generate a structural anomaly in the wafer that later becomes a fracture origin of wafer breakage. In our experience, such a breakage occurs during a final machining (cutting) process of the wafers, and a cross-section of the broken wafer is shown in Fig. 1. The size of the defect reaches a few hundred micrometers, a size comparable to the wafer thickness of 500 μm. In this wafer, many microdomains were found and also appear in Fig. I as straight channels throughout the wafer thickness. The defects were found on some of these microdomain channels. It should be noted that neither the microdomains nor the defects were detected in the virgin wafer and appeared only after it underwent a certain treatment (i.e., deposition and postannealing of the $SiO_2$ buffer layer).

Figure 2 is a secondary electron microscopic (SEM) image of the defect. As shown, the microdomain channel went through the defect. No impurities were detected in the chemical analyses via SEM; ions detected in these analyses were those heavier than beryllium. These facts suggest the possibility that the defect was caused by the generation of microdomains during wafer processing.

Figure 3 shows a similar defect found in another wafer on which an x-ray photoelectron spectroscopy (XPS) and an x-ray diffraction analysis (XRD) were performed. Figures 4(a) and 4(b) exhibit Nb 3*d* photoelectron peaks measured by micro-focused XPS of the defect and ordinary regions, respectively. The diameter of the focused x-ray beam was 1 50 μm. In order to remove surface

  

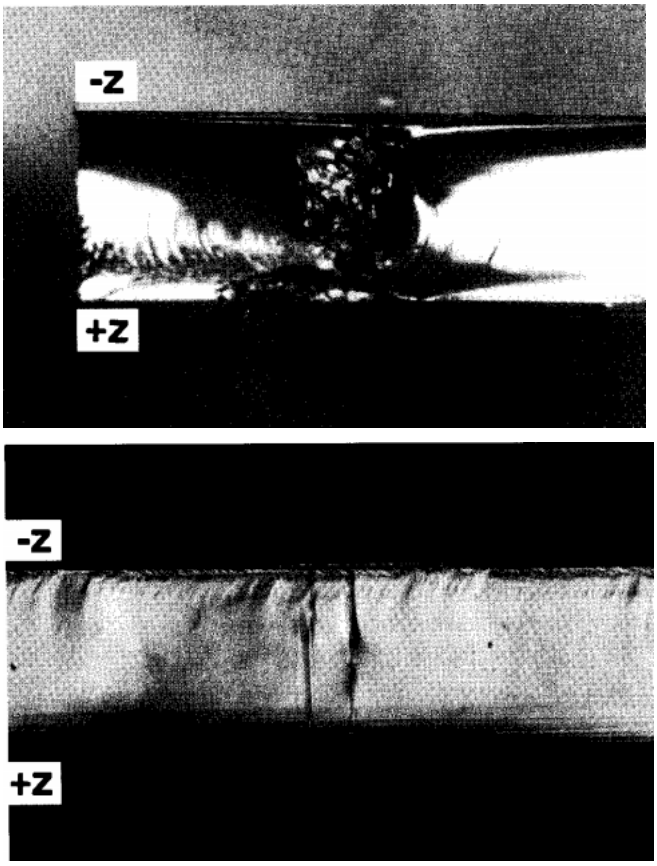


FIG. 1. Optical microscopic image of microdomains (lower) and defect on a microdomain that appeared on the fractured surface of an $LiNbO_3$ wafer. Thickness of the wafer is 500 μm.

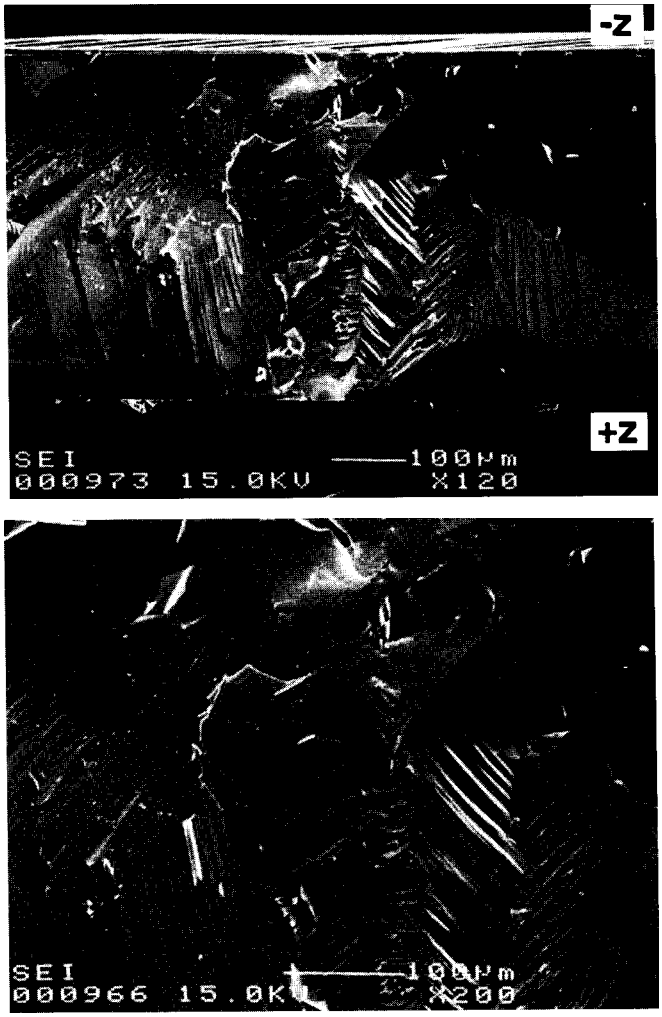


FIG. 2. SEM image of the defect in Fig. 1.

contamination before the analyses, the sample surface was lightly etched by Ar ions. From the ordinary regions [Fig. 4(b)], two pairs of Nb 3d peaks were detected and assigned to Nb ions of oxides; the peaks at 206.85 and 209.58 eV peaks are from $LiNbO_3$, and the other peaks at 204.77 and 208.11 eV are from NbO.[6] In contrast, peaks of metallic Nb were found from the defective region. In Fig. 4(a), the peaks at 204.28 and 207.15 eV are from NbO as well as those from the ordinary region, but the other peaks at 202.36 and 205.66 eV were attributed to metallic Nt).[6] Although it is possible that the ion etching before measurements caused chemically reduced Nb compounds such as NbO and metallic Nb, the complete absence of Nb ions from $LiNbO_3$ in the defective region is an anomalous fact. At the very least, the defect was caused by a chemical reaction accompanied by a reduction of the $LiNbO_3$. It should be noted that in the XPS analysis (from helium to uranium), no extrinsic impurities except for carbon were found in either the defective or the ordinary region.

A micro-XRD with a 100-μm-diameter Cu $K_\alpha$ beam was performed to examine the structure of the defect. Figure 5 is a comparison of XRD peaks of (a) the defective area and (b) those found in the ordinary region. Some extra peaks, marked by black circles, were detected from the defect, while all other peaks were assigned to the $LiNbO_3$ crystal . The XRD peaks from the defect are magnified in Fig. 6 with standard XRD peaks for $LiNbO_3$, LiH, LiD, and LiF. All the extra peaks can be assigned to the LiH. Because fluorine was not found in the XPS analysis, the existence of LiF was excluded as a possibility. Positions of other standard peaks for $LiNbO_3$-related compounds such as $LiNb_3O_8$, $Nb_2O_5$, and NbO were largely different from the position of the extra peaks. The possible existence of LiH is consistent with the fact that reduced Nb ions were found in the same defect by XPS.

Reportedly, LiH is stable under dry air atmosphere and melts at 680ºC.[7] Under this premise, the only possible explanation for the existence of LiH in the $LiNbO_3$ wafer is that it was formed after all of the high-temperature processes such as crystal growth, waveguide diffusion, annealing, etc., were finished. On the other hand, the

$LiNbO_3$ crystal contains a large amount of hydrogen ions as -OH even after the high-temperature processes.[8] Judging from the above examination results, we believe that the micro-repolarization occurring during the device fabrication process induced the local reduction of $LiNbO_3$ and the formation of LiH. Because the postprocessing repolarization is expected to occur explosively like a dielectric breakdown, it is plausible that the Li recombined with H in the $LiNbO_3$ crystal.

Microdomains, by themselves, do not weaken the mechanical strength of the LiNb03 wafer. However, as discussed above, when they are accompanied by a formation of a structural anomaly in the crystal, they could become the origin of fracture and greatly deteriorate the strength of the wafer. At this time, the observed structural anomaly (LiH) seemed not to generate a large stress inside of the wafer, because the wafers did not break until an external stress was applied by cutting wafers.

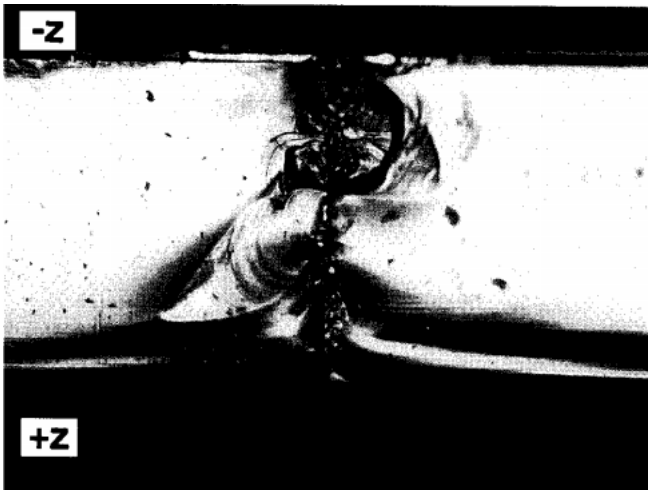


FIG. 3. Another example of a defect found on a microdomain. Thickness of the wafer is 500 μm.

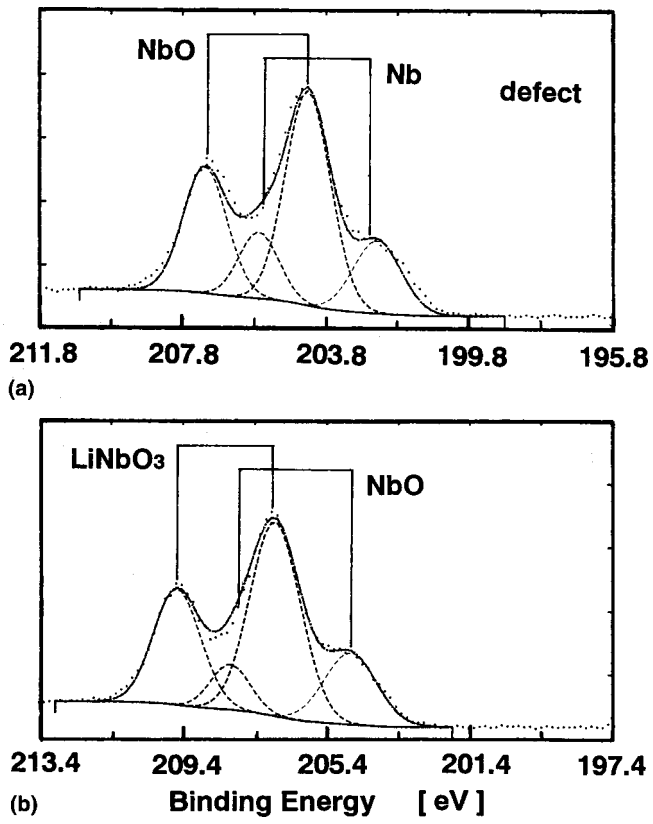


FIG. 4. XPS Nb 3*d* spectra measured for (a) the defect and (b) ordinary $LiNbO_3$.

## ACKNOWLEDGMENT

This work is supported by Special Coordination Funds for Promoting Science and Technology "Fundamental research on new materials of function-harmonized oxides," from the Japanese Science and Technology Agency.

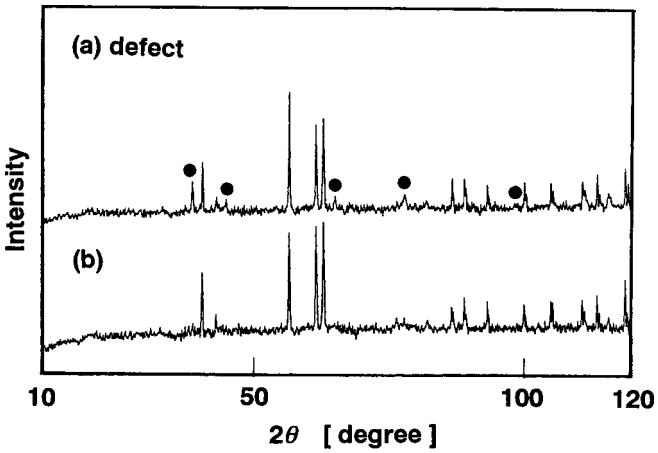


FIG. 5. XRD profiles measured for (a) the defect and (b) ordinary $LiNbO_3$.

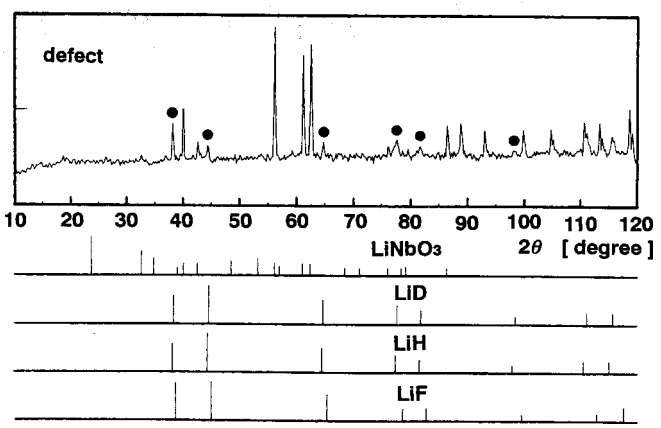


FIG. 6. XRD profile measured for the defect.

## REFERENCES


l. H. Nagata, N. Mitsugi, K. Higuma, J. Ichikawa, T. Sakamoto, T. Fujino, and T. Shinriki, in *Reliability of Photonics Materials and Structures*, edited by E. Suhir, M. Fukuda, and C.R. Kurkjian (Mater. Res. Soc. Symp. Proc. **531**, Warrendale, PA, 1998), p. 359.
2. F. Heismann, J. Lightwave Technol. **14**, 1801 (1996).
3. M.A. Powell and A.O. Donnell, Opt. Phot. News **8**, 23 (1997).
4. N. Mitsugi, H. Nagata, K. Shima, and M. Tamai, J. Vac. Sci. Technol. A **16**, 2245 (1998).
5. *Physics and Chemistry of Crystalline Lithium Niobate*, edited by A.M. Prokhorov and Y.S. Kuzminov (Adam Hilger, Bristol, England, 1990), Chap. 4.
6. *Handbook of Photoelectron Spectroscopy*, edited by J. Chastain (Perkin-Elmer, Eden Prairie~ MN, 1 992).
7. *Rihagaku-Giten (Handbook of Science)*, 4th ed. (Iwanarni Shoten, Tokyo, Japan, 1987).
8. H. Nagata, T. Sakamoto, H. Honda, J. Ichikawa, E.M. Haga, K. Shima, and N. Haga, J. Mater. Res. **11**, 2085 (1996).